

Article

Methane Cluster Fragmentation by Fast Electron Impact

Shuncheng Yan ^{1,2}, Ruitian Zhang ^{1,2} , Shaofeng Zhang ^{1,2} and Xinwen Ma ^{1,2,*} ¹ Institute of Modern Physics, Chinese Academy of Sciences, Lanzhou 730000, China² School of Nuclear Science and Technology, University of Chinese Academy of Sciences, Beijing 100049, China

* Correspondence: x.ma@impcas.ac.cn

Abstract: We investigate the fragmentation of the CH₄ cluster by fast electron impact at stagnation pressures from 0.5 bar to 16 bar. By measuring the time of flight spectrum (TOF), two types of ions, including (CH₄)_{n-1}CH₅⁺ and (CH₄)_{n-2}(C₂H_m)⁺, are observed. In the 1D TOF spectrum, it is shown that for the stagnation pressure larger than 4 bar, the former ion is predominant for each n, similar to the previous experimental result. However, as the pressure decreases to 0.5 or 2 bar, the contribution of the C₂H_m⁺ ion is dominant over that of the CH₄CH₅⁺ ion. In the 2D coincident TOF spectrum, the above two patterns of ions are also distinguished, and the enhancement of C₂H_m⁺ is observed at 4 bar pressure. The phenomena appearing in 2D and 1D TOF spectra imply that the C₂H_m⁺ ion prefers to survive in a smaller cluster, while the stabilization of the protonated ion needs a more massive cluster environment.

Keywords: methane cluster; mass spectrum; Coulomb explosion; reaction microscope

1. Introduction

Methane is a ubiquitous species widely existing in the interstellar cloud, young stellar objects, comets, and planetary systems [1–4], and is one of the main constituents of the atmosphere of Titan with an abundance of about 3% [5]. Since the low temperature of these environments, the formation of CH₄ cluster, CH₄ ice, or even CH₄ ocean is feasible. In recent years, fragmentation experiments involving CH₄ or its cluster have attracted a great deal of attention [6–21], which helps in understanding the formation mechanism of polycyclic aromatic hydrocarbons in the interstellar medium and the atmospheric chemistry of planets [6–10].

Several electron impact fragmentation experiments have been carried out for the methane cluster system [7,11–13], and two particular types of ions are involved: one is the protonated ion (CH₄)_{n-1}CH₅⁺ with n ≥ 1, starting from the outer shell electron ionization of CH₄; the other one is the (CH₄)_{n-2}(C₂H_m)⁺ ion with n ≥ 2 and m ≤ 7, whose prerequisite is the dissociative ionization or inner shell ionization of CH₄ to CH⁺, CH₂⁺, or CH₃⁺ ion. In the previous work, the incident energy has been limited to the low energy area from 12 to 70 eV, and the obtained relative contribution of (CH₄)_{n-2}(C₂H_m)⁺ ions was one order smaller than that of protonated ones.

In this work, we use an expansion nozzle with a smaller diameter. According to the scaling law [22], the cluster size decreases as a function of the nozzle diameter; thus, we could investigate the relative yield variation of the above two ions caused by the relatively small size of the cluster. We also raise the incident energy of the electron to 480 eV, which may cause the double or multiple ionization of the CH₄ cluster, emitting at least two charged fragments; we can then reconstruct the coincident map between the times of flight (TOF) of each ion, and investigate the yield ratio variation of (CH₄)_{n-2}(C₂H_m)⁺ to (CH₄)_{n-1}CH₅⁺ in the charged environment.



Citation: Yan, S.; Zhang, R.; Zhang, S.; Ma, X. Methane Cluster

Fragmentation by Fast Electron Impact. *Atoms* **2023**, *11*, 35. <https://doi.org/10.3390/atoms11020035>

Academic Editors: Izumi Murakami, Daiji Kato, Hiroyuki A. Sakaue and Hajime Tanuma

Received: 20 December 2022

Revised: 8 February 2023

Accepted: 8 February 2023

Published: 10 February 2023



Copyright: © 2023 by the authors. Licensee MDPI, Basel, Switzerland. This article is an open access article distributed under the terms and conditions of the Creative Commons Attribution (CC BY) license (<https://creativecommons.org/licenses/by/4.0/>).

2. Experimental Methods

This experiment is performed at the transversal reaction microscope at the Institute of Modern Physics, Chinese Academy of Sciences [23,24]. The main idea was proposed decades ago [25,26]. Briefly, the CH₄ molecular cluster is produced by the supersonic expansion of 20% methane gas seeded in Ar gas through a 30 μm nozzle at room temperature. In this adiabatic process, heat energy is converted to kinetic energy as the temperature of the clusters decreases to below 30 K. Colliding electron beam, with an energy of 480 eV and pulse width of 4 ns, interacts with the methane clusters in the reaction region from the direction both perpendicular to TOF electric field vector and cluster propagation vector. The collision impact ionization initiates the fragmentation of the CH₄ molecule and its cluster, and one or several charged ions will be emitted. During the 400 ns after the collision, a weak electric field of 2 V/cm is applied for the TOF spectrometer to avoid disturbing the electron beam. Then, the electric field is pulsed to 30 V/cm; under these interactions, the positive species are accelerated toward the ion position-sensitive detector. Based on the TOF information, we can deduce the mass of each ion.

In most cases, the cross-section of single ionization is one order higher than that of double ionization; this makes the single-ion emission event predominant, and its following dissociation decay pathways can be analyzed by using the 1D TOF spectrum. Alternatively, if double or multiple ionization happens, at least two charged ions will be produced. In our setup, the two ions are detected simultaneously, and via the coincident 2D TOF map, we can distinguish different decay pathways and investigate the intensity variation of each decay pathway as a function of the gas stagnation pressure (0.5 bar < *p* < 16 bar). In the offline analysis, we use the charged species of Ar⁺, Ar²⁺, Ar³⁺, Ar⁴⁺, and Ar⁵⁺ from the ionization of isolated Ar to calibrate our TOF spectrum, as lack of dissociation and intracluster reaction leads to the unambiguous identification of TOF positions for these ions.

We would point out that our experiment is not perfect, and some drawbacks have to be improved in the next step, even though they do not affect our conclusion in this work. Firstly, the utilization of the pulsed electric field, in particular, the weak electric field (2 V/cm during 400 ns after collision), significantly broadens the TOF peak of each ion, which causes poor mass resolution compared with previous work. Secondly, there is some residual gas in the reaction chamber, which induces two broad peaks around *m/z* = 160 amu. Thirdly, the heat dissipation of the pulsed power supply is not well; thus, the electric field drifts to some extent, and then it leads the TOF peak to deviate from the standard Gaussian shape; see the peak *m/z* = 40 amu in pressure of 0.5, 6 and 8 bar.

The drift of the electric field will not affect our analysis overall. On the one hand, the yield ratio of the byproduct to the total events is less than 5%, and the induced shape variation of the TOF peaks of C₂H_{*m*}⁺ and CH₄CH₅⁺ are not significant, as their original distributions are broad. On the other hand, the yield ratio of C₂H_{*m*}⁺ to CH₄CH₅⁺ is also not influenced since the TOF separation between these two ions is obviously larger than the time drift.

3. Results and Discussions

As shown in Figure 1, we begin the discussion from the 1D TOF spectrum; most of the observed ions arise from dissociation after single ionization of the CH₄ molecule or its cluster. In the low mass region smaller than 17 amu, several molecular species with *m/z* = 14, 15, and 16 amu could be assigned to the ions CH₂⁺, CH₃⁺, and CH₄⁺. As shown in the green rectangle, these three peaks are located at a broad background centered at 14 amu, extending over the 10–20 amu, which results mainly from the Coulomb explosion of multiply charged molecules and clusters. We did not observe notable variation in the relative yield and curve shape of this area as a function of cluster size. This means the relative number of clusters is small.

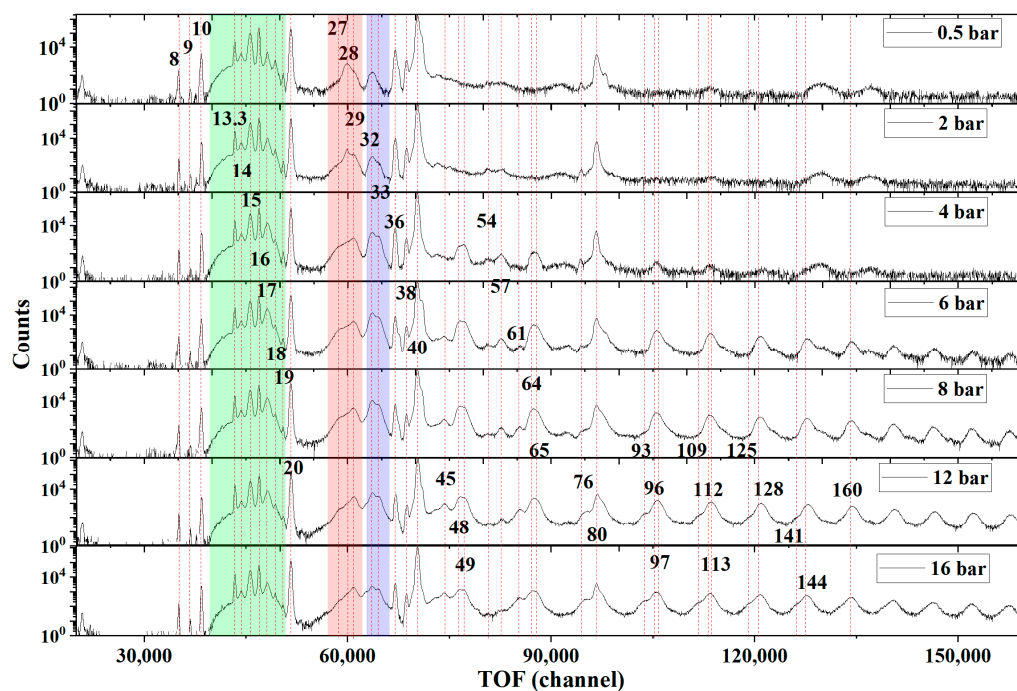


Figure 1. The 1D TOF spectrum of the ions after electron impact ionization as the stagnation pressure varies from 0.5 bar to 16 bar. The green rectangle shows the broad TOF distribution induced by the Coulomb explosion of the CH_4 ion; the red and blue rectangles indicate TOF distributions of the C_2H_m^+ ion and CH_4CH_5^+ ions, respectively; the dotted lines denote the m/z of each ion.

In the cluster region with m/z larger than 16, a peak at $m/z = 17$ amu is observed in all stagnation pressures; its relative yield to CH_4^+ is 3%, which is obviously higher than the yield ratio of $^{13}\text{CH}_4^+$ to $^{12}\text{CH}_4^+$ (1.1%). This peak is assigned to the protonated cluster ion CH_5^+ . At $m/z = 33$ amu, the CH_4CH_5^+ peak is also observed, and its yield is always smaller than that of CH_4CH_4^+ at 32 amu (see the blue rectangle in Figure 1). In the more massive cluster region, the peaks of $(\text{CH}_4)_{n-1}\text{CH}_5^+$ ion with $n \geq 3$ merge with the peak of $(\text{CH}_4)_n^+$ to form a broad peak, respectively, due to the resolution of our setup, thus preventing us from comparing their relative yield. The appearance of $(\text{CH}_4)_{n-1}\text{CH}_5^+$ ion is an indication of the protonation reaction, which is the subject of several papers in which a complex formation mechanism is involved. After a prompt collision between the incident electron and a methane molecule within the cluster, the ionization reaction generates a CH_4^+ ion and forms a $(\text{CH}_4)_k(\text{CH}_4\text{-CH}_4^+)$ species, followed by isomerization to the $(\text{CH}_4)_k(\text{CH}_3\text{-H-CH}_4^+)$ complex, which may later evolve into $(\text{CH}_4)_{n-1}\text{CH}_5^+$ cation ($n < k$) by loss of the CH_3 radical and CH_4 molecule. The CH_4 evaporation is due to that the formation of $(\text{CH}_4)_{n-1}\text{CH}_5^+$ is an exothermic process [7]. The excess energy should be released via the evaporation of the CH_4 molecule to cool the newly formed CH_5^+ ion. Obviously, if the parent cluster is not large enough, namely, smaller than the threshold size, the vibrational model may be excited and may quench the formation of the CH_5^+ ion.

In addition to peaks corresponding to $(\text{CH}_4)_{n-1}\text{CH}_5^+$ ions, a characteristic pattern of peaks $(\text{CH}_4)_{n-2}(\text{C}_2\text{H}_m)^+$ with $n \geq 2$ and $m \leq 5$ is clearly observed. For $n = 2$, three ions, including C_2H_3^+ , C_2H_4^+ , and C_2H_5^+ at 27, 28, and 29 amu, appear (see the red rectangle in Figure 1). For higher n , only the peak of $(\text{CH}_4)_{n-2}(\text{C}_2\text{H}_5)^+$ can be identified, while the other two peaks, including $(\text{CH}_4)_{n-2}(\text{C}_2\text{H}_4)^+$ and $(\text{CH}_4)_{n-2}(\text{C}_2\text{H}_3)^+$, are ambiguous due to the limitation of systematic resolution. The generations of such ions were proposed from the reaction between CH_4 and the ions CH^+ , CH_2^+ , or CH_3^+ after the dissociative ionization or inner shell ionization of the CH_4 molecule, as shown in several precedent experiments using photoionization and electron impact [7–13,27,28]. In their works, the $(\text{CH}_4)_{n-2}(\text{C}_2\text{H}_m)^+$ ions were observed as the minor decay pathway, and its cross-section is

approximately one order smaller than that of the $(\text{CH}_4)_{n-1}\text{CH}_5^+$ ion. In our experiment, for the pressure larger than 4 bar, the result is consistent with this observation. However, for $n = 2$, as the decrease of stagnation pressure, the contribution of the C_2H_m^+ ions increases gradually, which exceeds that of CH_4CH_5^+ at 2 bar, and reaches twice the latter one at 0.5 bar, as shown in the red and blue rectangles. This observation of the enhancement of C_2H_m^+ may imply that the C_2H_m^+ is more likely to survive in a relatively small cluster environment, while the stabilization of the CH_4CH_5^+ ion prefers a massive cluster.

One should note that the diameter of the nozzle in our experiment is $30\ \mu\text{m}$, which is much smaller than the $80\ \mu\text{m}$ in reference [7], and no precooling is being operated; thus, the overall cluster size should be smaller than that in the previous work under the same stagnation pressure. This is a distinctive characteristic of our experiment and may induce the enhancement of C_2H_m^+ ion. Additionally, carefully seeing the peak covering 27, 28, and 29 amu in the red rectangle, its overall shape also varies with the increase of the stagnation pressure, suggesting the relative intensity of C_2H_4^+ is significant in 0.5 bar and 2 bar. Nevertheless, in the higher pressure >4 bar, the other two types of ions, C_2H_3^+ and C_2H_5^+ , are major; this tendency suggests that a larger cluster favors stabilizing the latter two ions.

In Figure 2, we reconstruct the TOF1-TOF2 coincident map to display the flight-time correlation of two ions after the Coulomb explosion of the doubly-charged CH_4 cluster under 4, 6, and 16 bar, which is scarcely reported in the previous experiments.

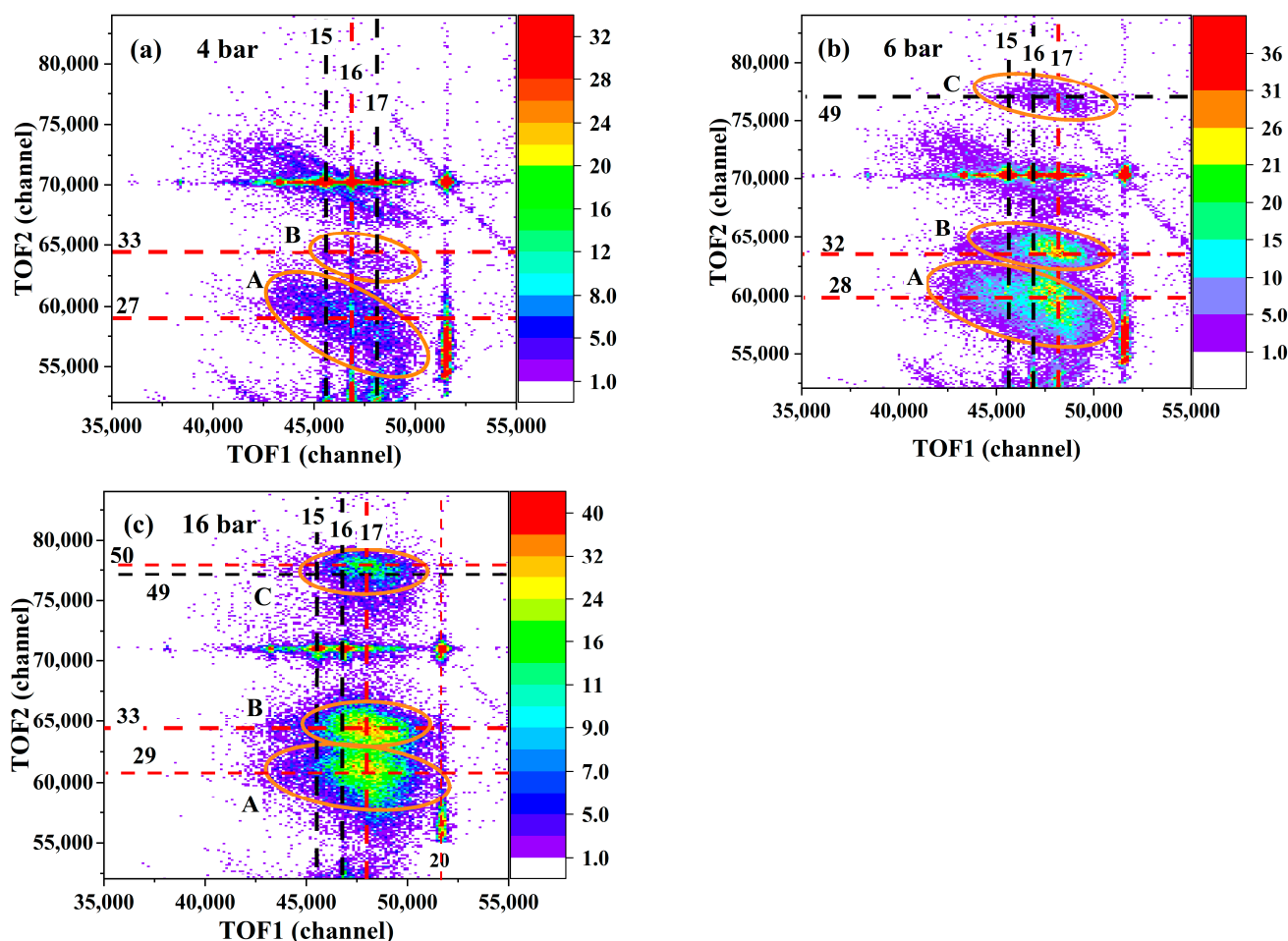


Figure 2. The 2D TOF spectrum of the ions after electron impact ionization at the stagnation pressure of (a) 4 bar, (b) 6 bar, and (c) 16 bar. Region A represents the $\text{CH}_4^+/\text{C}_2\text{H}_m^+$ or $\text{CH}_5^+/\text{C}_2\text{H}_m^+$ coincident island, while region B represents the $\text{CH}_4^+/\text{CH}_4\text{CH}_5^+$ or $\text{CH}_5^+/\text{CH}_4\text{CH}_5^+$ coincident island.

For the 2D TOF spectra in low stagnation pressure of 4 bar, as shown in Figure 2a, two regions marked by circle A and circle B are worth mentioning. For region A, the TOF of the first ion covers masses from $m/z = 15$ to 17 amu and is centered at 16 amu; this feature indicates the corresponding precursor ion does not reach the threshold size ensuring CH_5^+ formation through CH_3 and CH_4 evaporation but only causes the generation of CH_4^+ . The TOF center of the second ion lies around 27 amu representing the C_2H_m^+ ($m = 3$ or 4) ion. For region B, the center of the first ion locates around 16 amu, the same as region A, but the second ion shifts to $m/z = 33$ amu, suggesting the generation of CH_4CH_5^+ via protonation reaction.

Compared with the blue and red areas in Figure 1, the C_2H_m^+ and CH_4CH_5^+ ions are also simultaneously observed in Figure 2a, while the sole difference is the existence of neighboring CH_4^+ ion forming a charged environment. This allows us to study the relative production of these two types of ions in this environment.

We found that the intensity of region A in Figure 2a is dominant over that of region B. In more detail, by comparing the count rate of region A and region B, it is found that the yield ratio of the former one to the latter one is about 4.5; compared with the previous experimental result [7–13,27,28], this value increases a least one order. This phenomenon is similar to the observation of 1D TOF in 0.5 bar and 2 bar in Figure 1, where the contribution of C_2H_m^+ ion is also abundant. Therefore, the C_2H_m^+ ion is still easily generated from a light parent cluster ion under the low stagnation pressure condition, even though a neighboring CH_4^+ exists.

One should note that the Coulomb explosion makes the parent ion divide into two charged fragments; the size of the second ion after the Coulomb explosion should be essentially smaller than that of the initial parent ion before the Coulomb explosion; this is the reason we compare 2D TOF in 4 bar to 1D TOF in 2 bar and 0.5 bar.

For the larger pressure of 6 bar, as seen in Figure 2b, besides the yields of regions A and B increasing significantly, the TOF center of the first ion moves from 16 amu to 17 amu, forming a non-uniform bright coincident island. This indicates that the initial size of the first ion grows beyond the threshold size forming CH_5^+ via evaporation of CH_3 and CH_4 . Compared with Figure 2a, more events in region A of Figure 2b distribute together around the crossing point of $\text{CH}_5^+/\text{CH}_4\text{CH}_5^+$, indicating that the kinetic energy of the two ions becomes smaller as the cluster size increase.

For the highest stagnation pressure of 16 bar, as shown in Figure 2c, we find that the bright island in region A becomes even more intensive. Meanwhile, its covering range shrinks further, similar to that of region B. Especially, region B has similar intensity to region A. This suggests that, with the pressure increases, both C_2H_5^+ and the CH_4CH_5^+ will be enhanced in yield, but the latter channel obtains a higher priority.

Finally, we will highlight an interesting open question in this paper. Because of the limitation of our experimental condition, only the 1D TOF distribution and 2D TOF coincident map of the fragmentation products are measured, based on which we cannot identify the structure of the product ions and end the debate about whether the ion-molecular reaction could lead to the formation of a new type of covalent bond ions. On the one hand, in the previous fragmentation experiments of methane cluster, the TOF spectrum was used as the sole tool to identify the product species, which could not present the information on the internuclear distance between Carbon and Carbon atom in C_2H_m^+ ion; thus, one could not know whether this Van de Waals bond was converted into covalent bond during its isomerization, or it was kept as a weakly bound cluster ion. This is why several related experiments labeled the new ion as C_2H_m^+ ion rather than termed them ethylene ion, acetylene ion, or ethane ion. Recently, Leidlmair et al. [13] investigated the methane cluster fragmentation after electron impact by embedding it into a helium droplet, where the magic number effect of $(\text{CH}_4)_n(\text{C}_2\text{H}_m)^+$ was observed. They found that the magic number occurred at $n = 53$ for $(\text{CH}_4)_n\text{C}_2\text{H}_2^+$ and at $n = 54$ for $(\text{CH}_4)_n\text{C}_2\text{H}_4^+$, $(\text{CH}_4)_n\text{C}_2\text{H}_5^+$, $(\text{CH}_4)_n\text{C}_2\text{H}_6^+$, and $(\text{CH}_4)_n\text{C}_2\text{H}_7^+$. The difference was attributed to the lengths of these ions along the C–C covalent bond axis, therefore indicating the C–C bond formation. On

the other hand, the situation is different in the fragmentation experiment of the acetylene cluster, where the main emphasis was on the direct identification of bond conversion. By using the ion mobility spectroscopy, the produced ions $C_6H_6^+$ after cluster fragmentation are guided to pass through a gas cell; then, the ion-rare gas collision cross-section, the fragmentation products after the collision, and the flying time in the gas cell are obtained, which are all similar to the benzene ion; thus, the conversion from Van de Waals bond to covalent bond seems to be feasible [29–31]. Similarly, according to the quantum chemistry simulation, the generation of covalent $C_4H_4^+$ ions after single ionization of acetylene dimer could also be achieved [32]. In the future, in this important research field, we will analyze the structure and discuss the bond conversion rather than only be concerned with the TOF masses spectrum. Further or direct evidence may be supplied by the IR absorption spectrum.

4. Conclusions

In order to investigate the intracuster ion–molecule reaction, we performed the fragmentation of the CH_4 cluster by fast electron impact. By detecting ions using a reaction microscope, we reconstructed the 1D mass spectrum and 2D mass spectrum. The ion species including $(CH_4)_{n-1}CH_5^+$ and $(CH_4)_{n-2}(C_2H_m)^+$ ions are observed. In contrast with the larger stagnation pressure, where the yield of the $(CH_4)_{n-1}CH_5^+$ ion is relatively higher, in the 1D mass spectrum at 0.5 bar and 2 bar, an unusual feature is observed. We found that the $C_2H_m^+$ ion is abundant, which differs from previous electron impact and photoionization experiments. This observation indicates that the more massive cluster prefers the formation of the $CH_4CH_5^+$ by CH_3 or CH_4 evaporation. The relative yield enhancement of $C_2H_m^+$ ion is highlighted by using the nozzle with a smaller diameter in our experiment. Additionally, in the 2D mass spectrum, a similar change tendency is observed, as the pressure increases, both $C_2H_5^+$ and $CH_4CH_5^+$ ions are enhanced in yield, but the latter channel obtains a higher priority. This feature suggests that the charged environment is not vital to determine the decay mechanism.

Author Contributions: X.M. and S.Y. designed this experiment. S.Y. performed this experiment and wrote this manuscript. X.M., R.Z. and S.Z. read and commented on this manuscript. All authors have read and agreed to the published version of the manuscript.

Funding: This experimental work was supported by the National Natural Science Foundation of China under Grant No. U1832201, the Strategic Priority Research Program of the Chinese Academy of Sciences (XDB34020000). S. Y. wishes to acknowledge support from the Youth Innovation Promotion Association of the Chinese Academy of Sciences under Grant No. 2018448.

Data Availability Statement: Not applicable.

Conflicts of Interest: The authors declare no conflict of interest.

References

1. Boogert, A.; Gerakines, P.A.; Whittet, D.C. Observations of the icy universe. *Annu. Rev. Astron. Astrophys.* **2015**, *53*, 541. [[CrossRef](#)]
2. Gibb, E.; Mumma, M.; Russo, N.D.; DiSanti, M.; Magee-Sauer, K. Methane in Oort cloud comets. *Icarus* **2003**, *165*, 391. [[CrossRef](#)]
3. Qasim, D.; Fedoseev, G.; Chuang, K.J.; He, J.; Ioppolo, S.; van Dishoeck, E.F.; Linnartz, H. An experimental study of the surface formation of methane in interstellar molecular clouds. *Nat. Astron.* **2020**, *4*, 781. [[CrossRef](#)]
4. Formisano, V.; Atreya, S.; Encrenaz, T.; Ignatiev, N.; Giuranna, M. Detection of methane in the atmosphere of Mars. *Science* **2004**, *306*, 1758. [[CrossRef](#)]
5. Mousis, O.; Lunine, J.I.; Pasek, M.; Cordier, D.; Waite, J.H., Jr.; Mandt, K.E.; Lewis, W.S.; Nguyen, M.J. A primordial origin for the atmospheric methane of Saturn’s moon Titan. *Icarus* **2009**, *204*, 749. [[CrossRef](#)]
6. Molina-Cuberos, G.J.; López-Moreno, J.J.; Rodrigo, R.; Lara, L.M. Chemistry of the galactic cosmic ray induced ionosphere of Titan. *J. Geophys. Res. Planets* **1999**, *104*, 21997. [[CrossRef](#)]
7. Ding, A.; Cassidy, R.A.; Futrell, J.H.; Cordis, L. Ion-molecule reactions within methane clusters initiated by photoionization. *J. Phys. Chem.* **1987**, *91*, 2562. [[CrossRef](#)]
8. Herman, Z.; Henchman, M.; Friedrich, B. A beam scattering study of the dynamics of CH_4^+ (CH_4 , CH_3) CH_5^+ reaction in the eV collision energy range: Three competing mechanisms of CH_5^+ -formation. *J. Chem. Phys.* **1990**, *93*, 4916. [[CrossRef](#)]

9. Iwan, B.; Andreasson, J.; Bergh, M.; Schorb, S.; Thomas, H.; Rupp, D.; Gorkhover, T.; Adolph, M.; Möller, T.; Bostedt, C.; et al. Explosion, ion acceleration, and molecular fragmentation of methane clusters in the pulsed beam of a free-electron laser. *Phys. Rev. A* **2012**, *86*, 033201. [[CrossRef](#)]
10. Zaag, A.S.; Yazidi, O.; Jaidane, N.E.; Ross, M.W.; Castleman, A.W., Jr.; Al Mogren, M.M.; Linguerrri, R.; Hochlaf, M. Structure, reactivity, and fragmentation of small multi-charged methane clusters. *J. Phys. Chem. A* **2016**, *120*, 1669. [[CrossRef](#)]
11. Tian, C.; Vidal, C.R. Electron impact dissociative ionization and the subsequent ion-molecule reactions in a methane beam. *Chem. Phys.* **1997**, *222*, 105. [[CrossRef](#)]
12. Yi, H.; Kim, Y.; Choi, C.; Jung, K.-H. Intracluster ion–molecule reactions within methane homoclusters. *J. Mass Spectrom.* **1998**, *33*, 599. [[CrossRef](#)]
13. Leidlmair, C.; Bartl, P.; Schöbel, H.; Denifl, S.; Yang, S.; Ellis, A.M.; Scheier, P. Ionization of methane clusters in helium nanodroplets. *ChemPhysChem* **2012**, *13*, 469. [[CrossRef](#)] [[PubMed](#)]
14. Ren, X.; Pflüger, T.; Weyland, M.; Baek, W.Y.; Rabus, H.; Ullrich, J.; Dorn, A. High-resolution (e, 2e⁺ ion) study of electron-impact ionization and fragmentation of methane. *J. Chem. Phys.* **2015**, *142*, 174313. [[CrossRef](#)]
15. Field, T.A.; Eland, J.H. The fragmentation of CH₄⁺ ions from photoionization between 12 and 40 eV. *J. Electron. Spectrosc. Relat. Phenom.* **1995**, *73*, 209. [[CrossRef](#)]
16. Furuya, K.; Hayakawa, H.; Matsuo, A.; Ogawa, T. Translational energy distributions of excited CH⁺ ions produced by electron impact on methane. *J. Phys. B At. Mol. Opt. Phys.* **1999**, *32*, 621. [[CrossRef](#)]
17. Wolff, W.; Sigaud, L.; Montenegro, E.C.; de Jesus, V.L.B.; Cavasso Filho, R.L.; Pilling, S.; Santos, A.C.F. Ionization and Fragmentation of Methane Induced by 40 eV to 480 eV Synchrotron Radiation: From Valence to Beyond Core Electron Ionization. *J. Phys. Chem. A* **2013**, *117*, 56. [[CrossRef](#)]
18. Luna, H.; Cavalcanti, E.G.; Nickles, J.; Sigaud, G.M.; Montenegro, E.C. CH₄ ionization and dissociation by proton and electron impact. *J. Phys. B At. Mol. Opt. Phys.* **2003**, *36*, 4717. [[CrossRef](#)]
19. Sharifi, M.; Kong, F.; Chin, S.L.; Mineo, H.; Dyakov, Y.; Mebel, A.M.; Chao, S.D.; Hayashi, M.; Lin, S.H. Experimental and theoretical investigation of high-power laser ionization and dissociation of methane. *J. Phys. Chem. A* **2007**, *111*, 9405. [[CrossRef](#)]
20. Rajput, J.; Garg, D.; Cassimi, A.; Méry, A.; Flécharde, X.; Rangama, J.; Guillous, S.; Iskandar, W.; Agnihotri, A.N.; Matsumoto, J.; et al. Unexplained dissociation pathways of two-body fragmentation of methane dication. *J. Chem. Phys.* **2022**, *156*, 054301. [[CrossRef](#)] [[PubMed](#)]
21. Xu, S.; Ma, X.; Ren, X.; Senftleben, A.; Pflüger, T.; Dorn, A.; Ullrich, J. Formation of protons from dissociative ionization of methane induced by 54 eV electrons. *Phys. Rev. A* **2011**, *83*, 052702. [[CrossRef](#)]
22. Buck, U.; Krohne, R. Cluster size determination from diffractive He atom scattering. *J. Chem. Phys.* **1996**, *105*, 5408. [[CrossRef](#)]
23. Yan, S.; Zhang, P.; Stumpf, V.; Gokhberg, K.; Zhang, X.C.; Xu, S.; Li, B.; Shen, L.L.; Zhu, X.L.; Feng, W.T.; et al. Interatomic relaxation processes induced in neon dimers by electron-impact ionization. *Phys. Rev. A* **2018**, *97*, 010701. [[CrossRef](#)]
24. Yan, S.; Zhu, X.L.; Zhang, S.F.; Zhao, D.M.; Zhang, P.; Wei, B.; Ma, X. Enhanced damage induced by secondary high-energy electrons. *Phys. Rev. A* **2020**, *102*, 032809. [[CrossRef](#)]
25. Dörner, R.; Mergel, V.; Jagutzki, O.; Spielberger, L.; Ullrich, J.; Moshhammer, R.; Schmidt-Böcking, H. Cold target recoil ion momentum spectroscopy: A “momentum microscope” to view atomic collision dynamics. *Phys. Rep.* **2000**, *330*, 95. [[CrossRef](#)]
26. Ullrich, J.; Moshhammer, R.; Dorn, A.; Dörner, R.; Schmidt, L.P.H.; Schmidt-Böcking, H. Recoil-ion and electron momentum spectroscopy: Reaction-microscopes. *Rep. Prog. Phys.* **2003**, *66*, 1463. [[CrossRef](#)]
27. Smith, D.; Adams, N.G. Reaction of simple hydrocarbon ions with molecules at thermal energies. *Int. J. Mass Spectrom. Ion Phys.* **1977**, *23*, 123. [[CrossRef](#)]
28. Herman, Z.; Hierl, P.; Lee, A.; Wolfgang, R. Direct Mechanism of Reaction CH₃⁺ + CH₄ → C₂H₅⁺ + H₂. *J. Chem. Phys.* **1969**, *51*, 454. [[CrossRef](#)]
29. Momoh, P.O.; Abrash, S.A.; Mabrouki, R.; El-Shall, M.S. Polymerization of ionized acetylene clusters into covalent bonded ions: Evidence for the formation of benzene radical cation. *J. Am. Chem. Soc.* **2006**, *128*, 12408. [[CrossRef](#)]
30. Stein, T.; Bandyopadhyay, B.; Troy, T.P.; Fang, Y.; Kostko, O.; Ahmed, M.; Head-Gordon, M. Ab initio dynamics and photoionization mass spectrometry reveal ion–molecule pathways from ionized acetylene clusters to benzene cation. *Proc. Natl. Acad. Sci. USA* **2017**, *114*, E4125. [[CrossRef](#)] [[PubMed](#)]
31. Momoh, P.O.; El-Shall, M.S. Stepwise hydration of ionized acetylene trimer. Further evidence for the formation of benzene radical cation. *Chem. Phys. Lett.* **2007**, *436*, 25. [[CrossRef](#)]
32. Wang, Y.; Wang, E.; Zhou, J.; Dorn, A.; Ren, X. Formation of covalently bound C₄H₄⁺ upon electron-impact ionization of acetylene dimer. *J. Chem. Phys.* **2021**, *154*, 144301. [[CrossRef](#)] [[PubMed](#)]

Disclaimer/Publisher’s Note: The statements, opinions and data contained in all publications are solely those of the individual author(s) and contributor(s) and not of MDPI and/or the editor(s). MDPI and/or the editor(s) disclaim responsibility for any injury to people or property resulting from any ideas, methods, instructions or products referred to in the content.